

Designing 3-DOF Hardware-In-The-Loop Test Platform Controlling Multirotor Vehicles

Muhsin Hancer * Rahman Bitirgen ** Ismail Bayezit **

* Faculty of Aeronautical and Space Sciences, Necmettin Erbakan University, Konya, Turkey (e-mail: mhancer@konya.edu.tr)

** Faculty of Aeronautics and Astronautics, Istanbul Technical University, Istanbul, Turkey (e-mail: bitirgen@itu.edu.tr, bayezit@itu.edu.tr)

Abstract: Main idea of this paper is the development of Hardware-in-the-Loop test platform in order to flight mechanical modeling and better stabilization of multirotor vehicles via different feedback control structures, including PID controllers. First, nonlinear mathematical model of the quadrotor platform is built and validated via Matlab/Simulink based simulation environment. Then, Hardware-in-the-Loop (HIL) test scenario is developed to analyze and tune controller parameters with the help of in-house designed testbed mechanism. Next step is observing the quadrotor attitude maneuvers via embedded hardware over the gyroscopic gimbaled testbed. The HIL testbed enables us validate and calibrate model and control parameters within real-time environment including inertial and mechanical sensors for multirotor systems. In this study, the particular platform is IRIS cross-type quadrotor vehicle PID based control for stable hover flight.

Keywords: Hardware-in-the-Loop simulation, Model Based Design, Flight Mechanical Modeling, Engine Test Platform, Pixhawk Processor, Rotary Wing Aerial Vehicles, Multirotor Systems, Real-time PID Control.

1. INTRODUCTION

Recent developments on the sensor and electronics technology triggered increasing attention on the quadrotor air-vehicles. The usage of multirotor vehicles are increased very rapidly within civilian and military applications nowadays. Especially specific missions, which are dangerous for and over the capacity of humans, such as security and surveillance operations, detection and follow-up of enemies and targets, border patrolling, road traffic control, damage detection after natural disasters, investigation of crime scene, and agricultural applications.

In the literature, a lot of topics are studied for modeling and control of quadrotor vehicles. Before starting our HIL platform design task, our benchmarking is focused on testbench designs specifically for high fidelity and multi-physical modeling and control of quadrotor vehicles. Many researchers design various type of testbeds for experimental duties on the real-time stabilization of quadrotor vehicles. Prach et al. (2016) studies an experimental evaluation of the forward-propagating Riccati Equation control. The paper includes nonlinear dynamics of Quanser 3 Degrees of Freedom (3-DOF) Hover experimental testbench to update real-time feedback gains comparing with conventional linear quadratic regulator. Alexis et al. (2010) gives the background of design and verification of a constrained finite time optimal controller for attitude stabilization of a quadrotor embedded on the testbench. Experimental set-up consists of a fan for wind-gust disturbances and

Dragonfly quadrotor on-board Inertial Measurement Unit (IMU). Yu and Ding (2012) tests and validates 6-DOF flight controller on a quadrotor testbed. Quadrotor vehicle is mounted both 6-axes force/torque sensor (3-axes assigned to forces and 3-axes assigned to torques) and a sphere joint to let vehicle rotate in 3-axes. On-board IMU sensor is used for sensor fusion in order to experimentally control the vehicle via nonlinear trajectory linearization control technique. An et al. (2013) handles the control of a quadrotor vehicle using second order geometric sliding mode attitude observer on a testbench comparing traditional quaternion based sliding mode observer. The paper includes the design of an experimental testbed which composed of wireless reviver, on-board controller, and the IMU to stabilize of attitude states.

In this paper, a new 3-DOF HIL testbed is designed and manufactured at ITU Model Based Design Lab to test and validate different multirotor attitude maneuvers via tuning PID coefficients. Organization of this paper is as follows: Section 1 is the Introduction, includes the literature review and benchmarking of different HiL test platforms for multirotor operations. Section 2 presents mathematical modeling of cross-frame type quadrotor vehicle with Newton-Euler methods. Section 3 elaborates the identification of the quadrotor vehicle parameters considering frame type configuration with dimensions, motor and propeller thrust and drag coefficients, and experimental calculation of moments of inertia of quadrotor vehicle. Designing and manufacturing of HIL Aerospace testbed steps are also

expressed in this section. Simulation and implementation results are given in Section 4 related to the design of the quadrotor flight controller and the evaluation of simulations and experimental test results. Section 5 provides the conclusion discussing the potential future roadmap.

2. MATHEMATICAL MODEL OF CROSS TYPE QUADROTOR

Mathematical modeling of quadrotor is the prominent part in order to better design and tune controller gains. In this work, cross frame type IRIS quadrotor vehicle is used for simulation and experimental studies. Inertial, vehicle, and body frames can be considered as coordinate frames of quadrotor vehicle.

The inertial frame is earth centered at the vehicle motion starting point and has orthogonal three axes $\xi_i = (X_i, Y_i, Z_i)$. Vehicle frame is centered at center of gravity of the quadrotor $\xi_v = (X_v, Y_v, Z_v)$. This frame is used for translational motion of the vehicle with respect to inertial frame. The origin of the body coordinate frame, $\xi_b = (X_b, Y_b, Z_b)$ is related with rotational motion with respect to vehicle frame at the center of the gravity of the quadrotor. X axis points out to the front of the quadrotor with roll motion *phi* (ϕ) angle, Y axis always points out from right of the quadrotor with pitch motion *theta* (θ) angle and Z axis always points down from center of the gravity of the quadrotor with yaw motion *psi* (ψ) angle.

Quadrotor has two types of motion: linear translational and rotational motion. Quadrotor can also be represented as a point mass during translational motion for the sake of simplicity to obtain PID control gains. Linear and angular velocities are as follows:

$$\mathbf{V}_b = [u \ v \ w]^T$$

$$\mathbf{\eta}_b = [p \ q \ r]^T$$

Combination of three matrix to Direction Cosine Matrix to transform angular motion from body frame to inertial frame is obtained as (s refers to sine and c refers to cosine);

$$R_i^b = \begin{bmatrix} s\theta c\psi & c\psi s\theta s\phi - s\psi c\phi & c\psi s\theta c\phi + s\psi s\phi \\ s\theta s\psi & s\psi s\theta s\phi + c\psi c\phi & s\psi s\theta c\phi - c\psi s\phi \\ -s\theta & c\theta s\phi & c\theta c\phi \end{bmatrix}$$

$$R^b = R_i^b \cdot R^i$$

$$\begin{bmatrix} X^b \\ Y^b \\ Z^b \end{bmatrix} = \begin{bmatrix} s\theta c\psi & c\psi s\theta s\phi - s\psi c\phi & c\psi s\theta c\phi + s\psi s\phi \\ s\theta s\psi & s\psi s\theta s\phi + c\psi c\phi & s\psi s\theta c\phi - c\psi s\phi \\ -s\theta & c\theta s\phi & c\theta c\phi \end{bmatrix} \begin{bmatrix} X^i \\ Y^i \\ Z^i \end{bmatrix} \quad (1)$$

Rotational motion matrix for angular velocities in body frame;

$$\omega_b = R_\phi \begin{bmatrix} 0 \\ 0 \\ \dot{\phi} \end{bmatrix} + R_\phi R_\theta \begin{bmatrix} 0 \\ \dot{\theta} \\ 0 \end{bmatrix} + R_\phi R_\theta R_\psi \begin{bmatrix} \dot{\psi} \\ 0 \\ 0 \end{bmatrix} \quad (2)$$

$$\omega_b = \begin{bmatrix} \omega_{bx} \\ \omega_{by} \\ \omega_{bz} \end{bmatrix} = \begin{bmatrix} 1 & 0 & -s\theta \\ 0 & c\phi & c\theta s\phi \\ 1 & -s\phi & c\theta c\phi \end{bmatrix} \begin{bmatrix} \dot{\phi} \\ \dot{\theta} \\ \dot{\psi} \end{bmatrix}$$

Therefore, transformation of angular velocities from body frame to inertial frame is as follows;

$$\begin{bmatrix} \dot{\phi} \\ \dot{\theta} \\ \dot{\psi} \end{bmatrix} = \begin{bmatrix} 1 & s\phi t\theta & c\phi t\theta \\ 0 & c\phi & -s\phi \\ 1 & s\phi \frac{1}{c\theta} & c\phi \frac{1}{c\theta} \end{bmatrix} \begin{bmatrix} \omega_{bx} \\ \omega_{by} \\ \omega_{bz} \end{bmatrix} \quad (3)$$

$$T = -K_t(\omega_1^2 + \omega_2^2 + \omega_3^2 + \omega_4^2)$$

$$T = -K_t U_1 \quad (4)$$

T is total thrust of four motor and K_t is thrust coefficient of the propellers. U_1 is thrust control input.

$$\tau_\psi = -K_d(\omega_1^2 + \omega_2^2 - \omega_3^2 - \omega_4^2)$$

$$\tau_\psi = -K_d U_4 \quad (5)$$

K_d is drag coefficient of the propellers. U_4 is yaw control input.

$$\tau_\theta = -K_t(L_{xf}(\omega_1^2 + \omega_3^2) - L_{xb}(\omega_2^2 + \omega_4^2))$$

$$\tau_\theta = -K_t U_3 \quad (6)$$

$$\tau_\phi = -K_t(L_{yf}(\omega_3^2 - \omega_1^2) + L_{yb}(\omega_2^2 - \omega_4^2))$$

$$\tau_\phi = -K_t U_2 \quad (7)$$

U_2 and U_3 are roll and pitch control inputs. The following matrix shows relationship between control input and angular velocities of each motors with propeller coefficients.

$$\begin{bmatrix} T \\ \tau_\phi \\ \tau_\theta \\ \tau_\psi \end{bmatrix} = \begin{bmatrix} -K_t & -K_t & -K_t & -K_t \\ K_t L_{yf} & -K_t L_{yb} & -K_t L_{yf} & K_t L_{yb} \\ -K_t L_{xf} & K_t L_{xb} & -K_t L_{xf} & K_t L_{xb} \\ -K_d & -K_d & K_d & K_d \end{bmatrix} \begin{bmatrix} \omega_1^2 \\ \omega_2^2 \\ \omega_3^2 \\ \omega_4^2 \end{bmatrix} \quad (8)$$

Eq. (8) includes L_{yb} , L_{yf} , L_{xb} , and L_{xf} moment arms symmetric axis of X and Y as shown in Fig. 1.

The Gravity effect on the quadrotor direction is along to z axis into earth center. The vector notations of Gravity can be given as follows:

$$\mathbf{F}_G = \begin{bmatrix} 0 \\ 0 \\ mg \end{bmatrix} \quad (9)$$

The gravitational force acting on the quadrotors center of gravity in the body frame, it needs to be converted by multiplying the rotation matrix with the gravitational force vector in the inertia coordinate frame;

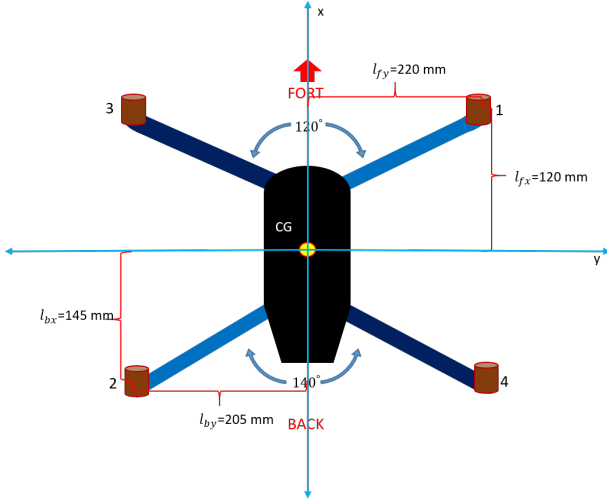


Fig. 1. Momentarm length and angles between arm groups of quadrotor.

$$\begin{aligned} \mathbf{F}_G^b &= \mathbf{P}_i^b \mathbf{F}_G^i \\ \mathbf{F}_G^b &= \begin{bmatrix} -mgs\theta \\ mgc\theta s\phi \\ mgc\theta c\phi \end{bmatrix} \end{aligned} \quad (10)$$

Force and Moment dynamic equations acting on the quadrotor are expressed as in Eq. (4–6) and Eq. (10). The basic principle of the Newton-Euler Method is given as:

$$\begin{bmatrix} \mathbf{F}^b \\ \boldsymbol{\tau}^b \end{bmatrix} = \begin{bmatrix} m\mathbf{I}_{3 \times 3} & \mathbf{0}_{3 \times 3} \\ \mathbf{0}_{3 \times 3} & \mathbf{I} \end{bmatrix} \begin{bmatrix} \dot{\mathbf{V}}^b \\ \ddot{\boldsymbol{\eta}}^b \end{bmatrix} + \begin{bmatrix} \dot{\boldsymbol{\eta}}^b \times (m\mathbf{V}^b) \\ \dot{\boldsymbol{\eta}}^b \times (\mathbf{I}\dot{\boldsymbol{\eta}}^b) \end{bmatrix} \quad (11)$$

Rotational equations with Newton-Euler method are as follows:

$$\begin{bmatrix} K_t \cdot U_2 \\ K_t \cdot U_3 \\ K_d \cdot U_4 \end{bmatrix} = \begin{bmatrix} I_{xx} \dot{\phi} \\ I_{yy} \dot{\theta} \\ I_{zz} \dot{\psi} \end{bmatrix} + \begin{bmatrix} qI_{zz}r - rI_{zz}q \\ rI_{xx}p - pI_{xx}r \\ pI_{yy}r - rI_{yy}p \end{bmatrix} \quad (12)$$

Translational equations with Newton-Euler method;

$$m \begin{bmatrix} \ddot{x} \\ \ddot{y} \\ \ddot{z} \end{bmatrix} = \begin{bmatrix} X^b \\ Y^b \\ Z^b \end{bmatrix} \begin{bmatrix} 0 \\ 0 \\ -K_t \cdot U_1 \end{bmatrix} + \begin{bmatrix} 0 \\ 0 \\ mg \end{bmatrix} \quad (13)$$

Nonlinear mathematical model of quadrotor with rotational and translational equations:

$$\begin{aligned} \ddot{x} &= (s\phi s\psi + c\psi s\theta c\phi) \frac{K_t U_1}{m} \\ \ddot{y} &= (-c\psi s\phi + s\psi s\theta c\phi) \frac{K_t U_1}{m} \\ \ddot{z} &= -g + (c\theta c\phi) \frac{K_t U_1}{m} \\ \ddot{\phi} &= \frac{I_{yy} - I_{zz}}{I_{xx}} qr + \frac{K_t U_2}{I_{xx}} \\ \ddot{\theta} &= \frac{I_{zz} - I_{xx}}{I_{yy}} pr + \frac{K_t U_3}{I_{yy}} \\ \ddot{\psi} &= \frac{I_{xx} - I_{yy}}{I_{zz}} qp + \frac{K_d U_4}{I_{zz}} \end{aligned} \quad (14)$$

3. PHYSICAL PARAMETER IDENTIFICATION OF QUADROTOR AND HIL TEST PLATFORM

Quadrotor physical parameter identification is divided into two phases in this section. First, motor and propeller thrust and drag coefficients are obtained for the calculation of thrusts and drag forces of the propelling mechanism with the help of in-house designed engine testbench as illustrated in Fig. 2. Next, moments of inertias (I_{xx} , I_{yy} , and I_{zz}) are calculated as the second of the experimental identification study.

3.1 Motor And Propeller Performance Testbed

Determining the physical parameters of the quadrotor vehicle needs special testbeds. These parameters are moments of inertia matrix, and propeller drag and thrust coefficients. Propeller coefficients are needed to calculate thrust, yaw, pitch and roll motion as seen in Eqs. (4–7). Therefore, obtaining K_t and K_d thrust and drag coefficients are pretty important.

Measurement of the thrust and drag are generated by the propeller. Thrust force is perpendicular to the rotation direction of the motor. The drag force generates moments around the rotation axis as seen in Figure 2. Basic formulations are $T = S \times (130/235)mm$ and $D = S \times (130/235)mm$. S is refer to scale reaction force. The thrust coefficient K_t and drag coefficient K_d formula are $K_t = T/\rho n^2 d^4$ and $K_d = D/\rho n^2 d^5$. n is refer to revolution per second (RPS), d is diameter of the propeller. So revolution per minutes (RPM) values is converted to RPS values to calculate K_t and K_d .

The motor-propeller performance testbed was designed on the CAD, produced with 3D printer assembled with T-motor MN 2213 950 Kv and 9.5×4.5 propellers. The motor were connected to Lipo Battery via a 20 Amp Electronic Speed Controller (ESC) unit and controlled by Arduino UNO with Pulse-Width modulation (PWM) signals.

There was some bottleneck when experimental works was going. Upstream flow is in front of the propeller that air flow encounters it. Downstream flow is back of the propeller that air flow passes it. First experiment, there was a blockage for downstream flow that acting as a ground effect that reducing the thrust nearly fifty percent and generated irritating sounds. Second experiment, the blockage was removed but when the gathering data in front of the propeller, thrust value was changing so upstream flow affects the thrust relatively. This aerodynamic experienced

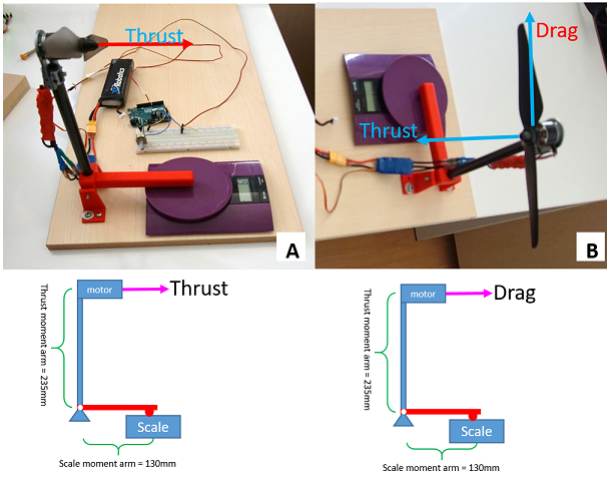


Fig. 2. A- Thrust Force, B- Drag Force Calculations.

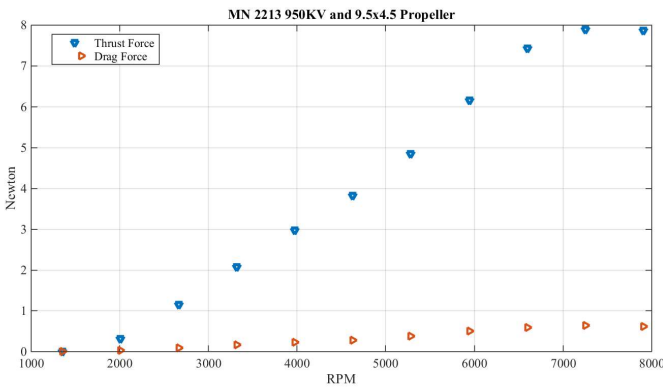


Fig. 3. Measurement thrust and drag values respect to RPM values.

was gained during the motor and propeller coefficients were experimented.

Experiment data consists of PWM, RPM, RPS and thrust or drag values as illustrated in Fig. 3. Thrust and drag experiments are done to get K_t and K_d coefficients.

3.2 Moments of inertia

The moment of inertia of the quadrotor is important for designing the controller and simulation. I_{xx} , I_{yy} and I_{zz} are calculated analytically and obtained experimentally. With assumption of symmetric geometry of the quadrotor, I_{xy} , I_{xz} , I_{yx} , I_{yz} , I_{zx} and I_{zy} are zero. Analytically calculations for same quadrotor model are used from Fum (2015), $I_{xx} = 0.0238kg.m^2$, $I_{yy} = 0.00882kg.m^2$, and $I_{zz} = 0.0303kg.m^2$. The obtaining the moments of inertias with experimental is a methodology that chronometer, ruler, scale and some rope are the basic needs. To preparing for the experimental set up, the quadrotor lash down along the desired moment of inertia axis. The ropes have to be lashed down perpendicular to the flat and parallel each others. To find I_{xx} and I_{yy} two rope is enough but for I_{zz} one more rope needs. Firstly, quadrotor is turned small angle enough to initiate oscillation on the center of mass along the desired axis. After oscillation and chronometer

Table 1. Moments of Inertia of Quadrotor

	Experimental	Analytical	Unit
I_{xx}	0.0218	0.0238	$kg \times m^2$
I_{yy}	0.0110	0.0088	$kg \times m^2$
I_{zz}	0.0301	0.0303	$kg \times m^2$

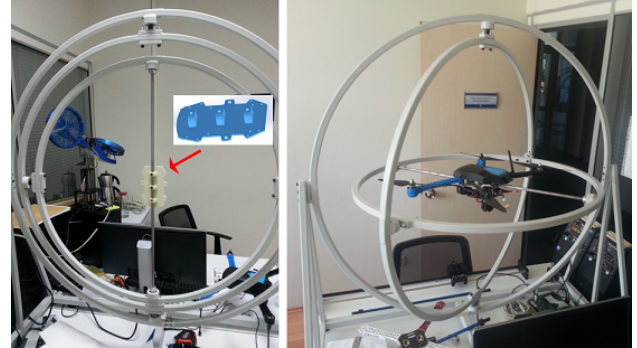


Fig. 4. The support part production and quadrotor assembly via support on the testbed.

are started same time, one coming and one going is counted one turn. Whenever it is felt enough then the period of the oscillation calculate with time (t) and turn counter (N), $T = t/N$. The eq. 15 is used to calculate moment of inertia. D refers to distance between ropes. L refers to length of ropes. g refers to gravity. m is mass of the quadrotor.

$$I = \frac{m \times g \times D^2 \times T^2}{16 \times \pi^2 \times L} \quad (15)$$

The experiment result is shown at the Table 1 with analytically results.

3.3 3-DOF Multirotor Test Platform

Validation of the simulation outputs is important before ready to flight. So experimental works are needed to verify how the control signal is reliability and stability. PID controller performance has to be tested on the testbench. Therefore, a new testbench is designed to implement control methods on the quadrotor vehicle with 3-DOF referring to attitude motions that are pitch, roll, and yaw. 3-DOF testbed having gyroscope working principle as main idea as in literature ?.

Main frame, outer circle, inner circle and beams materials were chosen as iron because of cheap, reachable and easily shaping and welding factors. Computer numerical control and iron bending machines were used at production process. Last step of producing was printing all the part with white color. Mounting the quadrotor model on the test platform is needed one part design and production. This parts should be at the center of mass of the quadrotor and the testbench and made from light material because of little affects on the quadrotor motion. The support part connecting the quadrotor on testbed was designed as CAD part then produced on the 3D (three dimensional) printer as seen in Fig. 4.

4. SIMULATION AND EXPERIMENTAL RESULTS

Quadrotor vehicle is dynamically modeled and HIL testbed is produced up to this section. The experimental identification of the quadrotor is done to run simulations and

implement on the HIL testbench via apply PID controller. Main aim of this section is PID controller responses both simulation and real time response of the quadrotor motions in the HIL testbed. This section composes of two main part. First is related with Matlab Simulink environment to run the nonlinear system models. Second is about to implementation of the designed PID controller real time C++ codes on the Pixhawk autopilot on the testbed and gathering the logged real flight data with manual tuning gains of the controllers. The main control architecture of this work is based on angle control via measured or simulated feedback signals. For attitude control of the quadrotor, HIL testbed was designed and simulations are run due to this perspective.

In this work, Pixhawk, controller of the system as hardware on board different types of sensors, controls the quadrotor system via designed control algorithm and sensors data to simulate HIL and validation. The Pixhawk runs the NuttX Shell real time operating system with Ardupilot open-source algorithms as software. On the HIL testbed, PID controller coefficients are manually set to reach optimal outputs. PID (Proportional-Integral-Derivative) controller is currently most used closed-loop (feedback) controller in industrial applications. Besides, simple structure and easily tuning the parameters and enabling efficiently and relatively robust control capabilities with regard to Modern Control Methods are attracting ways to be most in usage. It is currently been used to design autopilot for UAVs as a beginning for private sector companies and research institutes. Control architecture of quadrotor vehicle is in simulation environment is PID controller block and nonlinear model of quadrotor. There is an input to attitude controller block which includes both desired ϕ , θ , and ψ angles and outputs of feedback which are measured angles ϕ , θ , and ψ . In implementation, Pixhawk autopilot is used for real time tests.

4.1 PID Controller Simulation Result

In this work, Matlab Control System Toolbox is used for K_p , K_i , and K_d parameter of PID tuning for simulation of nonlinear model of quadrotor. During tuning each coefficient, others parameters values are get zero values to eliminate their effect on the tuned parameter.

Inputs of the simulation are set 20° for ϕ and θ angles but ψ is set 10° degree as seen in Figure 5. Both of the graphics have smaller than one second of rise time and 30% percent overshoot and 4 second settling time and have ignorable steady state errors. The nonlinearities of the system causes termination of simulation in short time. In shortly, the results shows that controlling of the quadrotor via PID controller is possible.

4.2 Experimental Real-Time Test Results

Two experiments are done on the HIL testbed with PID controller via different coefficients as seen in Tables 2 and 3. The response of the roll angle generally has some overshoots but rise and settling time is so small. About roll motions, there are ignorable overshoots and no time delay, so its so fast and robust. The pitch motions have no overshoots but some time delays and oscillations related

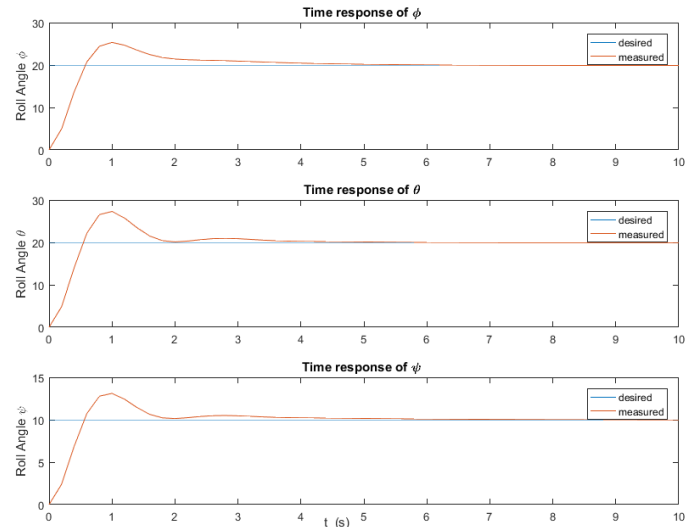


Fig. 5. Simulation results of PID controller on the nonlinear quadrotor model.

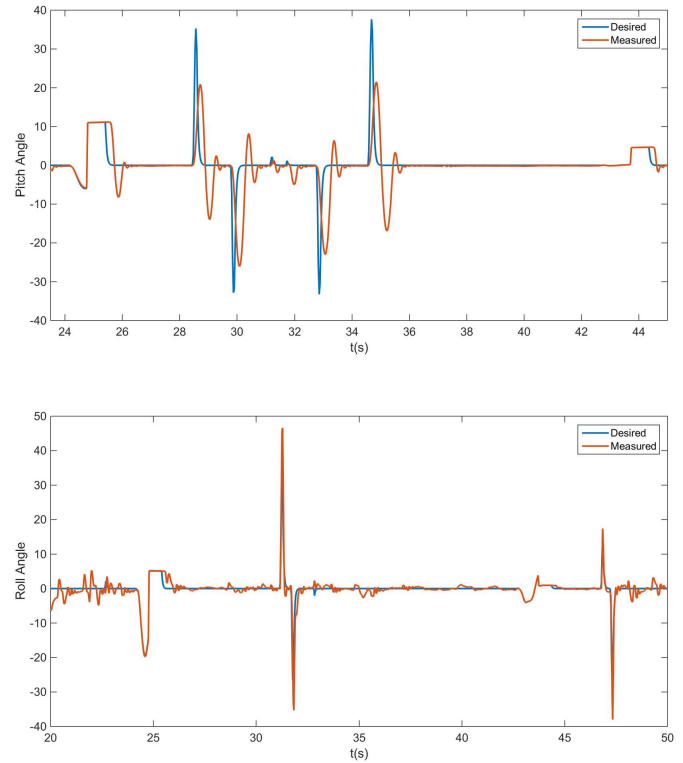


Fig. 6. Time responses of Pitch and Roll angles with respect to Table 2.

with moments of inertia. The yaw motions has high time delays and overshoots generated from high total moment of inertia from outer and inner circle of the testbench. Differences between first and second experiments are caused by P coefficient of PID controller. It is clearly seen that second experiment measured values of pitch angle is well tracking the reference signal than first experiment values. However, incrementation of P coefficient values on the roll angle causes some overshoot respected to first experiment. In addition, incrementation of P coefficient values on the yaw

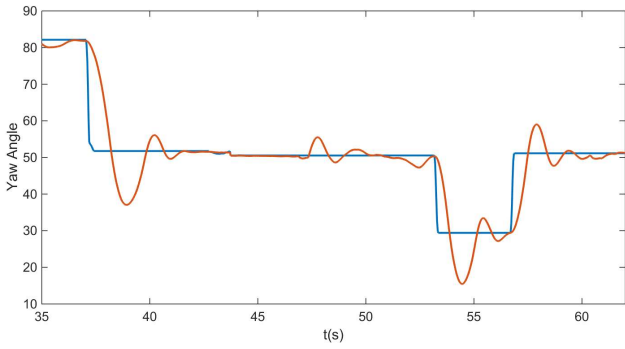


Fig. 7. Time response of Yaw angle with respect to Table 2.

angle decreases time delays on signal tracking respected to first experiment.

Table 2. PID Gains for First Experiment

	Roll Rate	Pitch Rate	Yaw Rate
K_p	0.3	3	2
K_i	0.09	0.09	0.018
K_d	0.0036	0.0036	0

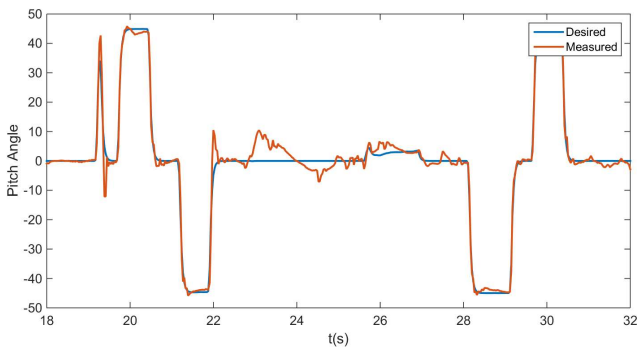


Fig. 8. Time response of Pitch angle with respect to Table 3.

Table 3. PID Gains for Second Experiment

	Roll Rate	Pitch Rate	Yaw Rate
K_p	0.4	4	0.35
K_i	0.09	0.09	0.018
K_d	0.036	0.0036	0

5. CONCLUSION

Testing aircraft controller performance is generally expensive and time consuming process due to hardship of flight operations. In this work, HIL testbed provides us easy solution in order to set optimum PID coefficients for quadrotor test platform. In the potential future roadmap, this platform enables us testing various nonlinear and robust controller structures, besides we are capable of testing the performance of tilt-rotor multicopter systems in the real-time test environment including inertial sensor information via Pixhawk controller. Especially feedback linearization, backstepping, and different nonlinear control approaches are still in progress. Additionally, we are still

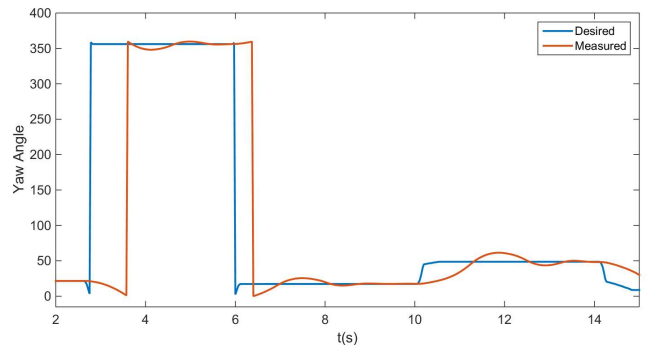
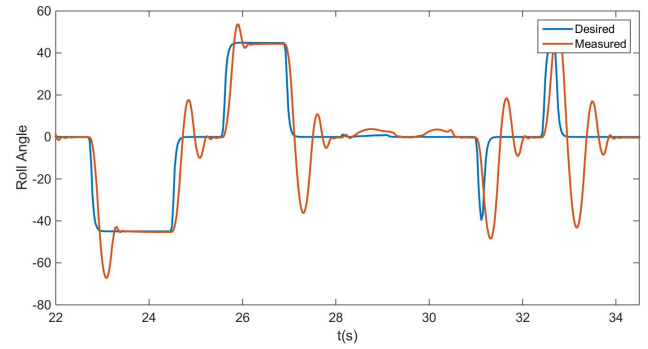


Fig. 9. Time Response of Roll and Yaw angles with respect to Table 3.

focusing on mitigating the inertial effects of outer rings and working on designing novel carbon-fiber based rings in order to provide minimum disturbance impact from gimballed platform.

REFERENCES

- Alexis, K., Nikolakopoulos, G., and Tzes, A. (2010). Design and experimental verification of a constrained finite time optimal control scheme for the attitude control of a quadrotor helicopter subject to wind gusts. In *Proceedings of IEEE ICRA'10 Robotics and Automation*, 1636–1641.
- An, H., Li, J., Wang, J., Wang, J., and Ma, H. (2013). Second-order geometric sliding mode attitude observer with application to quadrotor on a test bench. *Mathematical Problems in Engineering*, 2013.
- Fum, W.Z. (2015). *Implementation of Simulink controller design on Iris+ quadrotor*. Ph.D. thesis, Monterey, California: Naval Postgraduate School.
- Prach, A., Kayacan, E., and Bernstein, D.S. (2016). An experimental evaluation of the forward propagating riccati equation to nonlinear control of the quanser 3 dof hover testbed. In *Proceedings of IEEE American Control Conference*, 3710–3715.
- Yu, Y. and Ding, X. (2012). A quadrotor test bench for six degree of freedom flight. *Journal of Intelligent and Robotic Systems*, 1–16.